Light transport in photonic crystals composed of magneto-optically active materials

A. García-Martín and G. Armelles
Instituto de Microelectrónica de Madrid, Consejo Superior de Investigaciones Científicas, Isaac Newton 8, Tres Cantos, E-28760 Madrid, Spain

S. Pereira
Centre d'Optique, Photonique et Laser, Département de Génie Électrique et de Génie Informatique, Université Laval, Sainte-Foy, QC, Canada G1K 7P4

(Received 17 November 2004; revised manuscript received 10 February 2005; published 31 May 2005)

We analyze the properties of light propagation through ordered structures made of metallic wires (or disks) embedded in a dielectric medium in the presence of a magnetic field. The magnetic field not only modifies the polarization properties of the transmitted and reflected light, but it also induces absorption channels that give rise to well-defined structures in the transmission spectrum and in the Faraday rotation. Interaction and size effects are also analyzed. To perform the numerical simulations we extend an existing scattering matrix method to deal with the off-diagonal terms of the dielectric tensor required for the proper treatment of magneto-optical activity.

DOI: 10.1103/PhysRevB.71.205116 PACS number(s): 42.25.Bs, 42.70.Qs, 78.20.Ls

I. INTRODUCTION

The optical properties of periodically arranged nanostructures have received much attention in recent years. These structures, commonly called photonic crystals (PCs), can exhibit photonic band gaps in their dispersion relation or transmission spectrum. Most of the experimental and theoretical research concerning PCs has been confined to structures composed entirely of dielectric materials, where no light absorption takes place. However, structures fabricated with absorbing materials, such as metals, can also possess photonic band gaps; they can also exhibit spectral regions where light can propagate with almost no loss, despite the absorption of the metal. In particular, the photonic band structure of a two-dimensional array of metallic entities embedded in a dielectric medium has been calculated by several authors.[1–3] These studies have shown the existence of PC modes that originate from surface plasmon polaritons localized at the interface between the metallic and dielectric material. Surface plasmon polaritons are also present in nanostructured metallic layers, and are responsible for the extraordinary optical transmission observed in thin metallic films with an array of subwavelength holes.[4] In general, the optical characteristics of both of these types of metallic systems are established by the optical properties of the materials and the geometry of the structures, and cannot be varied once the structures are fabricated. However, in some applications it might be necessary to dynamically change the optical characteristics of the structure to control the flow of light, or the polarization state of the transmitted light. To do so requires the use of materials whose properties can be varied by external means such as electric fields (e.g., when liquid crystals are employed) or magnetic fields [e.g., magneto-optical (MO) active materials]. For instance, a magnetic field applied along the direction of propagation of a linearly polarized plane wave produces a rotation of the plane of polarization of the wave (Faraday rotation). Several studies have shown that in a one-dimensional PC containing MO materials such rotation can be strongly enhanced.[5,6] This enhancement is directly related to the localization of light in the PC as a result of the multiple interferences inside the structure. The effect has also been observed in the neighborhood of the stop-band of three-dimensional photonic colloidal crystals.[7] The magnetic field produces other effects such as the nonreciprocity of the dispersion relation $[\omega(k) \neq \omega(-k)]$, which leads to situations in which light can propagate in one direction but not in the opposite direction.[8,9] Furthermore, a magnetic field can be used to tune the position of the band gap of a PC.[10,11] All of these studies treated PCs constructed out of *dielectric* materials where at least one compound possessed MO properties.

The effect of the magnetic field on the behavior of plasmons in flat surfaces has been studied long ago[12] suggesting strong connections between the magnetic field and the plasmon propagation behavior. Very recently, nice results about the effect of the surface plasmon on the magnetic behavior of nanostructured gold thin film have also been put forward.[13] In this work we analyze the effect of a magnetic field on PC systems composed of both *metallic* and *dielectric* materials. We assume that the metallic portion of the system possesses MO activity, while the dielectric material does not. To the best of our knowledge such a study has not yet been presented, although some results on structures made on metallic films in the presence of a magnetic field have been put forward. For example, optical transmission through a metallic film with an array of subwavelength holes in the presence of a magnetic field applied in the film plane was analyzed theoretically in Ref. 14. In that study a strong dependence of the frequency of the extraordinary transmission peak on both the magnitude and direction of the in-plane component of the applied magnetic field was found. More recently, experiments on optical transmission through arrays of subwavelength holes fabricated on Co films have also been performed.[15] In that study, contrary to the case of photonic crystals made of dielectric materials,[4,5] the MO effects in the spectral range of the anomalous transmission band were much smaller than in nonperforated Co films. In the struc-

tures that we consider in this paper, the layers are made of metal wires or disks arranged periodically in a background dielectric material. We also assume that the amount of metal in each layer is much smaller than the amount of dielectric material (that is, the filling fraction of the metal is fairly small). Furthermore, in our study the magnetic field is applied perpendicular to the layer, and along the direction of the transmission of light. Such structures can be easily obtained by filling the pores of a porous alumina template, obtained by an anodization process from pure aluminium foils, with a MO active metal.[16] Under certain conditions the pores form an hexagonal arrangement[17] with a pore size and spacing in the nanometer range. These structures are relatively free from disorder over a range of several microns. Perfect hexagonal arrangements or even other geometries, can be obtained using in-print lithography.[18] To calculate the dispersion relation and optical transmission of the structures we use a scattering-matrix formalism developed by Whittaker and Culshaw,[19] which we have adapted to include the effects of the nondiagonal dielectric tensor that describes MO active materials.

The paper is organized as follows: first we present the case of a hexagonal arrangement of metallic wires/disks embedded in a dielectric medium when no magnetic field is applied. We discuss the effects of interactions due to the wire-to-wire distance on the dispersion curve of the layer and on the transmission through this layer. We then present our modified S-matrix formalism, and use it to analyze the effect of a magnetic field on the system. We conclude with a summary of the results presented.

II. INTERACTION EFFECTS ON THE DISPERSION CURVE AND ON THE OPTICAL PROPERTIES

For a single metallic wire embedded in a dielectric medium, the solution of Maxwell's equations in cylindrical coordinates (ρ,θ,z) gives rise to the following expression for the electric and magnetic fields for the mth mode:[20,21]

$$E_\rho = \left(\frac{iq}{K_j} Z_m^{j\prime}(K_j\rho)a_m^j - \frac{m\mu_j\omega}{K_j^2\rho} Z_m^j(K_j\rho)b_m^j\right)S_m,$$

$$E_\theta = \left(\frac{mq}{K_j^2\rho} Z_m^j(K_j\rho)a_m^j - \frac{i\mu_j\omega}{K_j} Z_m^{j\prime}(K_j\rho)b_m^j\right)S_m,$$

$$E_z = [Z_m^j(K_j\rho)a_m^j]S_m,$$

$$H_\rho = \left(\frac{m(K_j^2+q^2)}{\mu_j\omega K_j^2\rho} Z_m^j(K_j\rho)a_m^j - \frac{iq}{K_j} Z_m^{j\prime}(K_j\rho)b_m^j\right)S_m,$$

$$H_\theta = \left(\frac{i(K_j^2+q^2)}{\mu_j\omega K_j} Z_m^{j\prime}(K_j\rho)a_m^j - \frac{mq}{K_j^2\rho} Z_m^j(K_j\rho)b_m^j\right)S_m,$$

$$H_z = [Z_m^j(K_j\rho)b_m^j]S_m, \tag{1}$$

where q is the momentum in the direction of the wire and K_j represents the in-plane momentum, where $j=I,O$ labels the components inside (I) and outside (O) the cylinder. The function $Z_m^I(x)\equiv J_m(x)$ is the Bessel function of order n, and $Z_m^O(x)\equiv H_m^{(1)}(x)$ is the Hankel function of the first kind and order m. The prime denotes differentiation with respect to the argument $x=K_j\rho$. The quantities $K_j^2=\omega^2\epsilon_j(\omega)/c^2-q^2$ and $S_m=\exp(im\theta+iqz-i\omega t)$. The constants $a^{I,O}$ and $b^{I,O}$ must be determined by the boundary conditions. Applying the boundary conditions to the electric and magnetic field at the wire surface we obtain the dispersion relation for the different modes of the system.

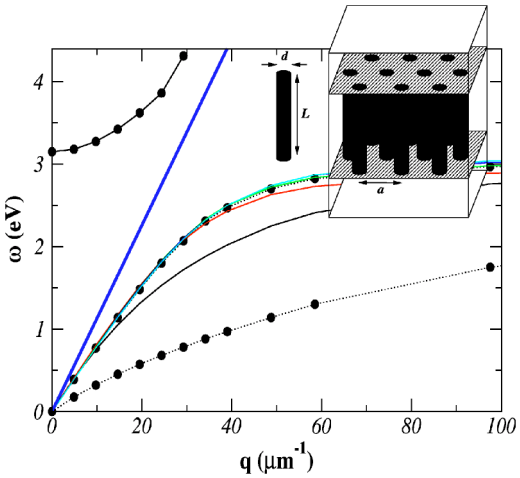

FIG. 1. (Color online) Dispersion relation of a infinitely long single wire. Dots correspond to a 10 nm diameter wire and thin lines to a 40 nm one. Inset, schematic view of the system under consideration.

In Fig. 1 we present the dispersion relation for an infinitely long metallic wire embedded in a background dielectric medium with index $n=1.75$. The dielectric constant of the wire is given by a Drude model,

$$\epsilon_{xx} = \epsilon_{yy} = \epsilon_{zz} = \left(1 + \frac{i\omega_p^2\tau}{\omega(1-i\omega\tau)}\right)\epsilon_\infty, \tag{2}$$

with $\tau=\infty$, $\omega_p=3.85$ eV, and $\epsilon_\infty=6.25$. The chosen parameter values (except τ) are similar to those of a metallike silver. The dots in Fig. 1 correspond to a wire with diameter $d=10$ nm, while the thin lines correspond to $d=40$ nm. For reference, we also show the so-called light line (thick solid line in Fig. 1), that is, the dispersion curve corresponding to a plane wave propagating in a medium with a refractive index equal to that of the background dielectric medium. The branches located on the right-hand side of the light line represent modes that have a purely imaginary in-plane momentum K_O, and are thus strongly localized near the wire-dielectric interface.[21] The modes located on the left-hand side of the light line have a real in-plane momentum K_O, and thus spread deeply into the background dielectric, but remain finite for $\rho=\infty$.

The PC system that we analyze in this paper is depicted schematically in the inset of Fig. 1. It consists of a periodic arrangement of wires embedded in a dielectric medium. Interaction effects between adjacent wires can potentially play a large role, leading to a dispersion relation markedly differ-

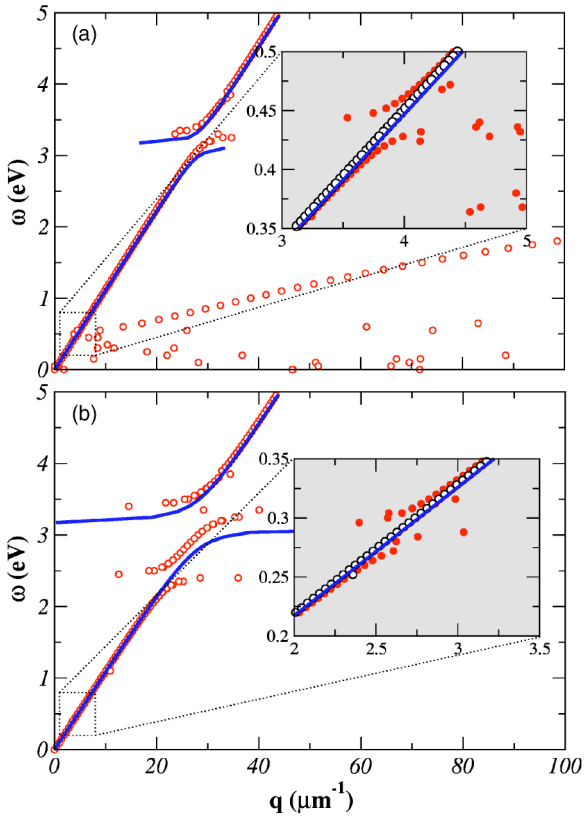

FIG. 2. (Color online) (a) Dispersion relation of a hexagonal array (lattice parameter $a=100$ nm) for wires with 10 nm in diameter. Open circles $\omega_c=0$ eV, filled circles $\omega_c=0.04$ eV, we have used $\tau=\infty$. Thick solid line corresponds to the MG approximation. (b) The same as (a) but for an array with $a=50$ nm. Insets, detailed view of the low frequency range.

ent to that presented in Fig. 1. Furthermore, we note that for a single wire the solutions to Maxwell's equations that give rise to electromagnetic field distributions divergent for ρ infinite, where ρ is the distance from center of the cylinder, are discarded, because they have no physical significance. However, in our system such solutions must be considered, since they are primarily responsible for the wire-to-wire interaction, which may lead to new classes of physically significant modes. In Fig. 2 we present the dispersion relation of a periodic hexagonal arrangement of wires with the same wire diameter ($d=10$ nm) as that of Fig. 1, but with a wire-to-wire spacing of $a=100$ nm (a) and $a=50$ nm (b). As mentioned, these curves were obtained using a scattering matrix formalism,[19] which we have modified to describe the nondiagonal dielectric tensor required for the description of MO activity. In Fig. 2 the open circles represent the case where no magnetic field is applied, while the filled circles give the case where a weak magnetic field, characterized by a cyclotron frequency $\omega_c=0.04$, is applied. In fact, because the magnetic field is weak, the difference between the open circles and the filled circles is not evident, except in the insets of Fig. 2. In the remainder of this section we concentrate on the results with *no* applied magnetic field (open circles). In the following section we will consider the applied magnetic field, and give the details of our modifications to the scattering matrix formalism.

There are some important differences between the dispersion relation of a single wire (Fig. 1) and the dispersion relation of the metallic PC (Fig. 2). First, we observe the appearance of modes whose dispersion relation almost follows a straight line. This is because for a wide range of energies (wavelengths) both the wire diameter and the wire-to-wire distance are much smaller than the wavelength of light, so the medium (wires+matrix) can be seen as an homogeneous medium characterized by an effective index of refraction. This is unlike Fig. 1, where the dispersion relation is always different than the light line. To quantify the extent to which the PC structure can be described by a homogeneous medium we display the dispersion curve (thick solid line) obtained by using a Maxwell-Garnett effective medium approach for the system (wires+matrix).[22] This effective medium approach reproduces some of the features observed in the dispersion curve calculated using the scattering matrix (SM) formalism, the feature at about 3.2 eV, and, to some extent, the slope of the dispersion relation away from 3.2 eV. The feature at 3.2 eV corresponds to a surface plasmon mode of the wires, similar to the modes already reported in Refs. 1–3. However, there are other effects that are not reproduced by the effective medium model, such as the extra branch of modes appearing in the infrared region (0–2 eV) of Fig. 2(a). Furthermore, the Maxwell-Garnett approximation does not account for the effects of wire-to-wire interaction. For example, in Fig. 2(b), where the wires are spaced by 50 nm, the feature at 3.2 eV displays *two* splittings instead of the one splitting observed in Fig. 2(a), when the wires are spaced by 100 nm. We note that for the sake of clarity we have removed the second branch of modes in the infrared region of Fig. 2(b). The two splittings in Fig. 2(b) come from the fact that the distance between the wires has been reduced, and thus the interactions between the surface plasmon modes increase, giving rise to new couplings.

To analyze the transport properties of the system along the wire axis, we have calculated the transmission of light in a system where the thickness of the wire layer is $L=200$ nm. We use the same parameter values as for Fig. 2, except that we now set $\tau=6$ eV^{-1} in order to get a more realistic situation ($\tau=\infty$ eV^{-1} gives anomalously sharp peaks). The refractive index of the incident and substrate medium is taken to be equal to the refractive index of the background dielectric medium in the wire layer. In Fig. 3 we plot the transmission through the structure for a wire spacing of $a=218$ nm (a), $a=100$ nm (b), and $a=50$ nm (c). The open circles in (a)–(c) represent the case where no magnetic field is applied, while the thin lines represent the case where a magnetic field characterized by $\omega_c=0.04$ eV, is applied. Again, in this section we concentrate on the case with no magnetic field applied.

For a wire-to-wire distance of $a=218$ nm [Fig. 3(a)], the transmission spectrum exhibits a single dip centered at ~3.6 eV. Since there is only one dip, we conclude that it corresponds to the situation where a surface plasmon mode is excited in each wire, but the individual modes interact only minimally with each other. However, when we reduce the wire-to-wire distance to $a=100$ nm (b), which corresponds to the dispersion relation in Fig. 2(a), we note that the transmission dip has shifted to ~3.2 eV, with a small shoulder at ~3.8 eV. We attribute this shift and the appearance of the

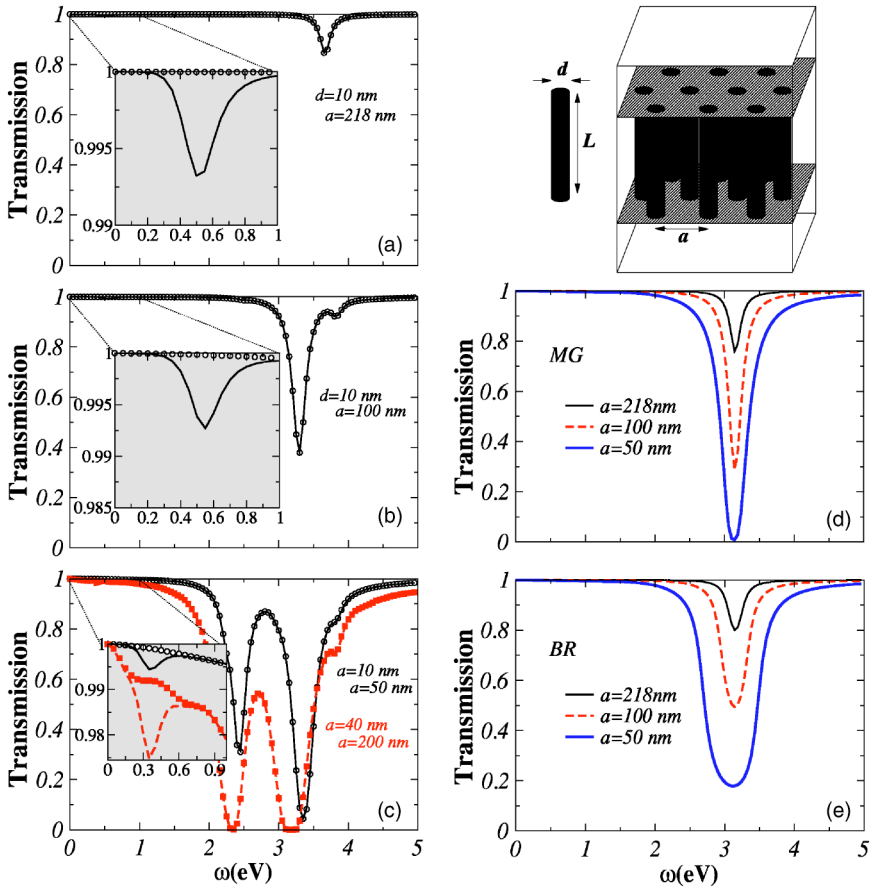

FIG. 3. (Color online) Transmission as a function of the frequency for *s*-polarized light at normal incidence and for $\tau = 6\ \mathrm{eV}^{-1}$. (a) $d = 10$ nm, $L = 200$ nm, $a = 218$ nm wires for $\omega_c = 0$ eV (open circles) and $\omega_c = 0.04$ eV (thin lines). Inset, detailed view of the low frequency range. (b) The same as in (a) but for $d = 10$ nm, $L = 200$ nm, $a = 100$ nm wires (circles and thin solid lines for $\omega_c = 0$ eV and $\omega_c = 0.04$ eV, respectively). (c) The same as in (a), (b) but for $d = 10$ nm, $L = 200$ nm, $a = 50$ nm wires (circles and thin solid lines for $\omega_c = 0$ eV and $\omega_c = 0.04$ eV, respectively) and for $d = 40$ nm, $L = 800$ nm, $a = 200$ nm (squares and dashed lines). (d) Transmission spectra using a MG effective medium for concentrations of 0.2% (thin solid line), 0.9% (dashed line), and 3.6% (thick solid line). The aspect ratio d/L is 0.5 for all three curves as well as the thickness that is $L = 200$ nm. (e) The same as (d) but using the BR approach.

shoulders to the beginning of interactions between the surface plasmon modes of the different wires. When we decrease the wire-to-wire distance to $a = 50$ nm (c) we substantially enhance the surface plasmon interaction, and consequently we observe two extremely deep dips, which correspond to the features in the dispersion relation in Fig. 2(a).

For the sake of comparison we present transmission spectra calculated using two different effective medium approximations, a perturbative approach [Fig. 3(d)], where the metallic wires slightly modify the dielectric tensor of the background dielectric medium [Maxwell-Garnet (MG) approximation]; and a self-consistent model [Fig. 3(e)] where the background dielectric medium and the metallic wires are treated on the same footing [the so-called Bruggemant (BR) approximation].[23] The spectra were calculated for the three different wire concentrations obtained from the three wire-to-wire distance considered above. Both approximations predict only one transmission dip, but the two differ in their relationship between the strength of the dip and the wire-to-wire spacing. In the MG approximation the dip broadens slightly, and shifts towards lower energies as the concentration increases. However, in the BR approximation the dip broadens considerably, and the shift towards lower energies is larger than in the MG approximation. These behaviors (broadening + shift) reflect the increasing interactions between the metallic wires. Nevertheless, since both approximations essentially model a *random* (i.e., nonperiodic) distribution of wires, they are not able to reproduce the splitting induced by surface plasmon interaction. Only when the wire-to-wire distance is large do the effective medium models give similar results to the results of the scattering matrix simulations.

In Figs. 4(a) and 4(b) we present the calculated transmission spectra for an hexagonal array of metallic disks embedded in the same dielectric matrix as in the case of the wires. These spectra were obtained for a disk diameter of $d = 10$ nm and for a disk-to-disk distance of (a) $a = 100$ nm and (b) $a = 50$ nm. The thickness of the disk layers was $L = 2$ nm, which gives an aspect ratio (d/L) of 5 (for the wires the aspect ratio was 0.05). Apart from the decrease of the signal due to the reduction of the thickness of the metallic elements, we observe several effects; first, there is an overall redshift of the dips with respect to the case of the wires. This is purely geometrical effect, induced by the change in the aspect ratio. Second, the spectra have a richer structure than in the case of the wires. This reflects the dependence of the interactions between the surface plasmons on the shape of the structures. In Fig. 4(d) we present the transmission spectra obtained using a MG approximation [in the BR approximation a similar result is obtained, except for the aforementioned broadening of the peak, more pronounced in this case, as shown in Fig. 4(e)]. Here only one dip is obtained, which originates from the surface plasmon of the disk. This dip is located at lower energy than the dip that originates from the surface plasmon of the wires. The spectra display a stronger dependence on the metallic concentration for the disks than for the wires.

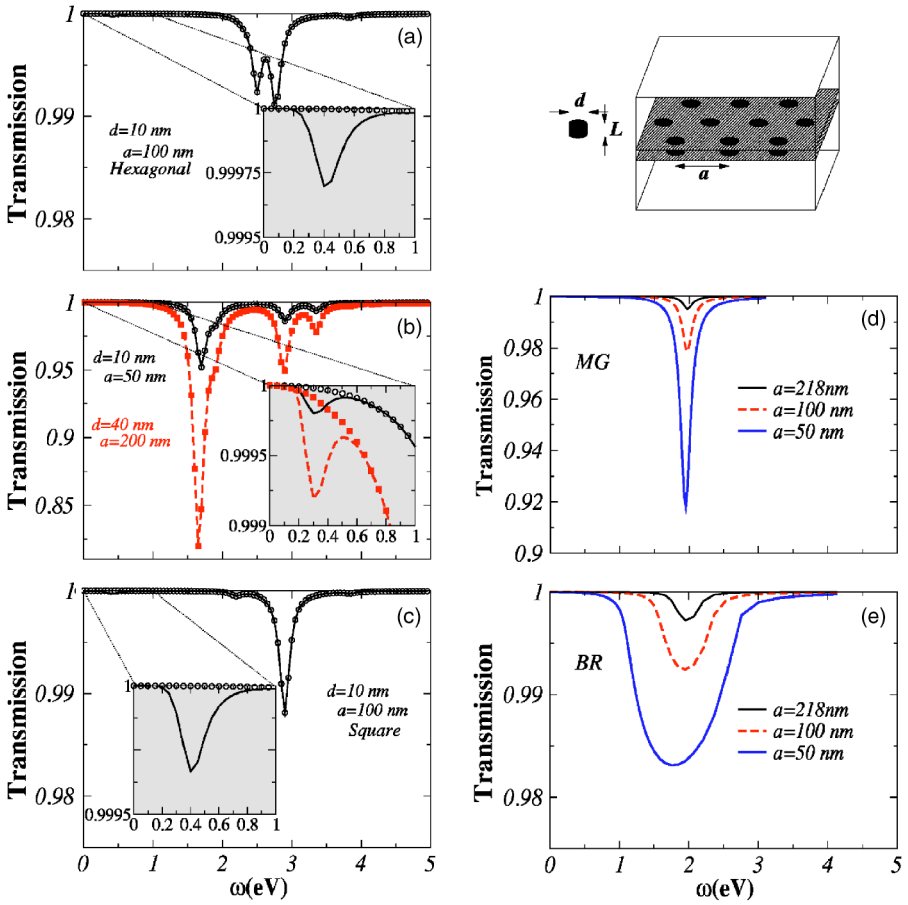

FIG. 4. (Color online) Transmission as a function of the frequency for *s*-polarized light at normal incidence and for $\tau = 6\ \mathrm{eV}^{-1}$. (a) $d=10$ nm, $L=2$ nm, $a=100$ nm disks for $\omega_c=0$ eV (open circles) and $\omega_c=0.04$ eV (thin lines). (b) The same as in (a) but for $d=10$ nm, $L=2$ nm, $a=50$ nm disks (circles and thin solid lines for $\omega_c=0$ eV and $\omega_c=0.04$ eV, respectively) and for $d=40$ nm, $L=8$ nm, $a=200$ nm (squares and dashed lines). (c) The same as in (a) but for a square array of disks. Insets, detailed view of the low frequency range. (d) Transmission spectra using a MG effective medium for concentrations of 0.2% (thin solid line), 0.9% (dashed line), and 3.6% (thick solid line). The aspect ratio d/L is 5 for all the curves as well as the thickness that is $L=2$ nm. (e) The same as (d) but using the BR approach.

For wire-to-wire or disk-to-disk distances small enough to exhibit strong interactions, the transmission spectra depend also on the geometry of the arrangement. This is shown in Fig. 4(c) where the transmission spectrum of a square array of disks with $d=10$ nm and $a=100$ nm is shown. A comparison with Fig. 4(a) reflects that there is not only a shift in the position of the dips, but also a change in the overall structure of the spectrum.

The position of the dips presented in Figs. 3 and 4 also depends on the diameter of the wire (or disk). As we increase the diameter we observe a shift of the peak (or peaks) towards lower energy and also the appearance of peaks for larger diameters [see squares in Fig. 3(c) and Fig. 4(b)]. Such finite size effects have also been observed in other nanostructures.[24]

III. MAGNETIC FIELD EFFECTS

We now consider a dc magnetic field applied along the wire axis (or perpendicular to the plane of the disk) and assume that the effect of the applied magnetic field on the background dielectric medium is negligible. The dielectric tensor of the wires, described by the Drude model, takes the form

$$\epsilon = \begin{pmatrix} \epsilon_{xx} & \epsilon_{xy} & 0 \\ \epsilon_{yx} & \epsilon_{yy} & 0 \\ 0 & 0 & \epsilon_{zz} \end{pmatrix}, \quad \eta \equiv \epsilon^{-1} = \begin{pmatrix} \eta_{xx} & \eta_{xy} & 0 \\ \eta_{yx} & \eta_{yy} & 0 \\ 0 & 0 & \eta_{zz} \end{pmatrix}, \quad (3)$$

where

$$\epsilon_{xx} = \epsilon_{yy} = \left(1 + \frac{i(1-i\omega\tau)\omega_p^2\tau}{\omega[(1-i\omega\tau)^2+\omega_c^2\tau^2]}\right)\epsilon_\infty,$$

$$\epsilon_{zz} = \left(1 + \frac{i\omega_p^2\tau}{\omega(1-i\omega\tau)}\right)\epsilon_\infty,$$

$$\epsilon_{xy} = -\epsilon_{yx} = \frac{i\omega_c\omega_p^2\tau^2}{\omega[(1-i\omega\tau)^2+\omega_c^2\tau^2]}\epsilon_\infty, \quad (4)$$

where ω_c is the cyclotron frequency, and the rest of parameters have the same definition as in the preceding section.

To numerically simulate the effects of the magnetic field on our metallic PC we again use the scattering matrix formalism developed by Whittaker and Culshaw.[19] However, in their formalism they assumed that the dielectric tensor was diagonal with $\epsilon_{xx}=\epsilon_{yy}=\epsilon_{zz}$. To account for the effects of the magnetic field we need a formalism that treats dielectric tensors of the form of Eq. (3). To do so we change Eq. (3.5) of Ref. 19 to

$$\left\{\begin{pmatrix} \hat{\eta}_{yy} & -\hat{\eta}_{yx} \\ -\hat{\eta}_{xy} & \hat{\eta}_{xx} \end{pmatrix}\left[\begin{pmatrix} q^2 & 0 \\ 0 & q^2 \end{pmatrix} + \begin{pmatrix} \hat{k}_x\hat{k}_x & \hat{k}_x\hat{k}_y \\ \hat{k}_y\hat{k}_x & \hat{k}_y\hat{k}_y \end{pmatrix}\right] + \begin{pmatrix} \hat{k}_y\hat{\eta}_{zz}\hat{k}_y & -\hat{k}_y\hat{\eta}_{zz}\hat{k}_x \\ -\hat{k}_x\hat{\eta}_{zz}\hat{k}_y & \hat{k}_x\hat{\eta}_{zz}\hat{k}_x \end{pmatrix}\right\}\begin{pmatrix} \phi_x \\ \phi_y \end{pmatrix} = \omega^2\begin{pmatrix} \phi_x \\ \phi_y \end{pmatrix}, \quad (5)$$

where $\hat{\eta}_{ij}$ represents the matrix containing the Fourier expan-

sion of η_{ij}, $\hat{k}_i$ is a diagonal matrix with elements $\hat{k}^i_{\mathbf{GG}}=k_i+G_i$, and G_i is a reciprocal lattice vector in the direction $\vec{i}$, and ϕ_i are vectors ($\phi_i=[\phi_i(\mathbf{G}_1),\phi_i(\mathbf{G}_2),\ldots]^T$) containing the plane wave expansion as that of Ref. 19. We consider dielectric tensors that satisfy $\eta_{xx}=\eta_{yy}$ and $\eta_{yx}=-\eta_{xy}$, which permits the following definition:

$$\mathcal{H}\equiv\begin{pmatrix}\hat{\eta}_{yy} & -\hat{\eta}_{yx}\\ -\hat{\eta}_{xy} & \hat{\eta}_{xx}\end{pmatrix}=\begin{pmatrix}\hat{\eta}_{xx} & \hat{\eta}_{xy}\\ -\hat{\eta}_{xy} & \hat{\eta}_{xx}\end{pmatrix}=\mathcal{E}^{-1} \tag{6}$$

which, after defining

$$K\equiv\begin{pmatrix}\hat{k}_x\hat{k}_x & \hat{k}_x\hat{k}_y\\ \hat{k}_y\hat{k}_x & \hat{k}_y\hat{k}_y\end{pmatrix}, \tag{7a}$$

$$\mathcal{K}\equiv\begin{pmatrix}\hat{k}_y\hat{\eta}_{zz}\hat{k}_y & -\hat{k}_y\hat{\eta}_{zz}\hat{k}_x\\ -\hat{k}_x\hat{\eta}_{zz}\hat{k}_y & \hat{k}_x\hat{\eta}_{zz}\hat{k}_x\end{pmatrix}, \tag{7b}$$

$$\phi\equiv\begin{pmatrix}\phi_x\\ \phi_y\end{pmatrix}, \tag{7c}$$

leads to the required eigenvalue equation for the momentum q, i.e., the analogue to Eq. (3.7) of Ref. 19,

$$[\mathcal{E}(\omega^2-\mathcal{K})-K]\phi=q^2\phi. \tag{8}$$

Using this eigenvalue equation with our definitions, we can directly apply the formalism of Ref. 19 to obtain the fields and the transmission and reflection coefficients associated with a metallic PC structure in the presence of a magnetic field. Both the background medium and the cylinders can, in principle, be metallic with a given magneto-optical activity. However, in this paper we confine ourselves to the situation where the background medium is purely dielectric, and non-MO active, while the metallic cylinders embedded in the background dielectric medium are MO active.

We first analyze the modification that the magnetic field induces in the dispersion curves of the patterned layer. We will consider very weak magnetic fields, namely $\omega_c=0.04$ eV. This value of ω_c corresponds to a MO activity similar to that observed in Co. The results are given by the filled circles in Fig. 2. Since the magnetic field is very small, on the large scale of the figure there is essentially no difference when the magnetic field is applied (note that the open circles lie exactly on top of the filled ones). However, a detailed look at the low frequency range (see insets in Fig. 2) clearly reveals the effect of the nondiagonal terms of the dielectric tensor of the wires. For both values of the wire-to-wire diameter a new splitting of the light line is present when a magnetic field is applied. This modification of the dispersion curve has its consequence in the transmission spectrum, as shown in the insets in Fig. 3 where we observe the appearance of a peak at low energies. For a fixed value of the wire-to-wire spacing the intensity of this peak increases linearly with the magnetic field and shifts to higher energies as ω_c increases. On the other hand, if we fix the value of the magnetic field and vary the wire-to-wire spacing, the position and intensity of the peak varies in a similar way as for the high energy peak, although here no splitting was observed. This peak is also present in the disk layers (see insets Fig. 4), with the same characteristics regarding its position and magnetic field dependence as those observed in the wire case. It is remarkable that the low frequency mode does not appear in any of the effective medium models.

The origin of this feature comes from the interactions between the modes appearing on a single wire when a magnetic field is applied.[25] In the case of a single wire the modes whose intensity outside the wire decrease when the distance to the origin increases are located around ω_c for large q. However, those solutions with increasing amplitude (that do not have physical meaning for a single wire) are located at a higher value of the frequency and in them lies the origin of the features observed in the low frequency range of the spectrum.

As we have just mentioned, the application of a magnetic field along the axis of the wires (or perpendicular to the disks) produces a modification of the state of polarization of the transmitted or reflected light. The numerical method that we use allows us to directly calculate the conversion from *s*-polarized light into *p*-polarized light. In other words, the polarization *rotation* both in reflection (Kerr) and in transmission (Faraday) induced by the nondiagonal term of the dielectric tensor can be obtained. Since the incoming light is considered to be at normal incidence, the polarization conversion is purely a consequence of the fact that $\epsilon_{xy}\neq 0$.

Our calculation of the Faraday rotation of the metallic PC structure is depicted in Fig. 5 for a hexagonal arrangement of wires (disks in the inset) with a spacing of $a=100$ nm (a). We choose $\omega_c=0.04$ eV, and all other parameters are the same as for Fig. 3. The regions of strong Faraday rotation correlate perfectly with the transmission dips in Fig. 3(b) and Fig. 4(a). Again, for the sake of comparison we present the Faraday rotation calculated using the two effective medium approximations discussed above.[26] The intensity of the Faraday rotation for PC structure is weaker than that predicted by either effective medium approach, both for wires and disks (note that both curves for the patterned medium have been scaled by a multiplicative factor). This could indicate that the periodic ordering in the PC structure induces a decrease of the polarization conversion due to collective effects, resulting in a decrease of the Faraday rotation. A remarkable issue is the low frequency region, where the signal for disks is larger than that of the high frequency region, in clear opposition to the intensity of the transmission spectrum for the same parameters. The effect is not related to the enhancement of the MO activity in photonic crystals, since there the effect is due to multiple interferences induced by the localization of the wave due to the band gap properties inherent to these materials.

We also present results for a wire-to-wire spacing of $a=50$ nm Fig. 5(b). The general situation is the same as for the larger wire-to-wire spacing of Fig. 5(a). However, the relative intensities of the peaks for the disks are now different: the low frequency signal is smaller than the high frequency one. This behavior was not noticeable when we analyzed the transmission spectrum, showing that the Faraday rotation is more sensitive to changes in the concentration of MO active materials. In the case of the wires this effect is also present, but the decrease in the relative intensity is smaller.

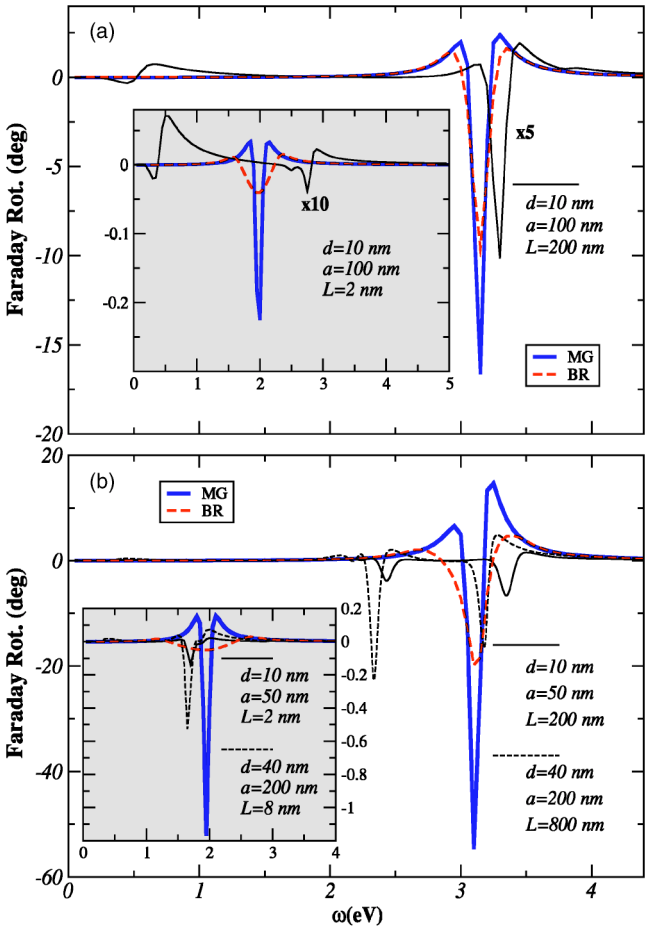

FIG. 5. (Color online) Faraday rotation as a function of the frequency for *s*-polarized light at normal incidence and for $\tau = 6\ \mathrm{eV}^{-1}$. (a) $d = 10$ nm, $L = 200$ nm, $a = 100$ nm wires for $\omega_c = 0.04$ eV (thin lines). Inset, the same for $L = 2$ nm disks. Thick solid lines (thick dashed lines) are the result considering the corresponding MG (BR) effective medium (i.e., 0.9% concentration and aspect ratios of 0.5 for wires and 5 for disks). (b) The same as in (a) but for $d = 10$ nm, $L = 200$ nm, $a = 50$ nm wires (thin solid line) and for $d = 40$ nm, $L = 800$ nm, $a = 200$ nm (thin dashed lines). Inset, the same for $L = 2$ nm (thin solid line) and $L = 8$ nm disks (thin dashed line). The concentration is in this case 3.6%.

IV. SUMMARY

To sum up, we have analyzed the transport properties of light through a patterned medium, when the propagation is in the direction of the axis of the cylinders/disks of the structure. To perform the analysis we have extended an existing scattering matrix method to allow for the presence of off-diagonal terms in the dielectric tensor. We have addressed the problem of light transmission through a hexagonal array of metallic cylinders/disks presenting a combination of plasmonlike structures and magneto-optical terms. This combination gives rise to couplings that cannot be treated within a traditional effective medium theory but that are accurately described by the microscopic scattering matrix formalism. The infrared part of the spectrum exhibit clear magnetic-field induced couplings that can be of great utility in the framework of sensors and biosensors. The behavior of the structures as a function of the concentration of metallic substances has also been discussed, revealing interesting size effects. We have also pointed out that the infrared structures appear also in the Faraday rotation but showing an interesting concentration sensitivity. The large differences found between the effective medium (not accounting for order effects) and the patterned one for all the cases studied suggest that the collective effects occurring in well ordered, periodic media result in an inhibition of the polarization conversion giving rise to a decrease of the Faraday rotation.

ACKNOWLEDGMENTS

This work was partially financed by the E.U. under Nanomagic Contract No. IST-2001-33186. The authors also acknowledge financial support from the Spanish MEC through the program Ramón y Cajal (A.G.-M.) and to the MCyT through Grant No. MAT2002-04484 and CAM through Grant No. 07N/0108/2002. One of the authors (S.P.) acknowledges support from the Natural Sciences and Engineering Research Council of Canada (NSERC).

[1] V. Kuzmiak and A. A. Maradudin, Phys. Rev. B **58**, 7230 (1998).
[2] T. Ito and K. Sakoda, Phys. Rev. B **64**,045117 (2001).
[3] E. Moreno, D. Erni, and C. Hafner, Phys. Rev. B **65**, 155120 (2002).
[4] T. W. Ebbesen, H. J. Lezec, H. F. Ghaemi, T. Thio, and P. A. Wolff, Nature (London) **391**, 667 (1998).
[5] M. Inoue, K. I. Arai, T. Fujii, and M. Abe, J. Appl. Phys. **85**, 5768 (1999).
[6] M. J. Steel, M. Levy, and R. M. Osgood, Jr., J. Lightwave Technol. **18**, 1297 (2000).
[7] C. Koerdt, G. L. J. A. Rikken, and E. Petrov, Appl. Phys. Lett. **82**, 1538 (2003).
[8] A. Figotin and I. Vitebsky, Phys. Rev. E **63**, 066609 (2001).
[9] A. Figotin and I. Vitebsky, Phys. Rev. B **67**, 165210 (2003).
[10] A. Figotin, Y. A. Godin, and I. Vitebsky Phys. Rev. B **57**, 2841 (1998).
[11] M. S. Kushwaha and G. Martinez, Phys. Rev. B **65**, 153202 (2002).
[12] R. F. Wallis, J. J. Brion, E. Burstein, and A. Hartstei, Phys. Rev. B **9**, 3424 (1974); R. L. Stamps and R. E. Camley, *ibid.* **31**, 4924 (1985); J. W. Wu, P. Hawrylak, G. Eliasson, and J. J. Quinn, *ibid.* **33**, 7091 (1986).
[13] I. I. Smolyaninov, C. C. Davis, V. N. Smolyaninova, D. Schaefer, J. Elliott, and A. V. Zayats, Phys. Rev. B **71**, 035425 (2005).
[14] Y. M. Strelniker and D. J. Bergman, Phys. Rev. B **59**, R12763 (1999).

[15] M. Diwekar, V. Kamaev, J. Shi, and Z. V. Vardeny, Appl. Phys. Lett. **84**, 3112 (2004).
[16] M. S. Martín-González, A. L. Prieto, R. Gronsky, T. Sands, and A. M. Stacy, Adv. Mater. (Weinheim, Ger.) **15**, 2003 (2003).
[17] H. Masuda and K. Fukuda, Science **268**, 1466 (1995).
[18] J. Choi, J. Schilling, K. Nielsch, R. Hillebrand, M. Reiche, R. B. Wehrspohn, and U. Gösele, Mater. Res. Soc. Symp. Proc. **722**, L5.2 (2002).
[19] D. M. Whittaker and I. S. Culshaw, Phys. Rev. B **60**, 2610 (1999).
[20] C. A. Pfeiffer, E. N. Economou, and K. L. Ngai, Phys. Rev. B **10**,3038 (1974).
[21] U. Schröter and A. Dereux, Phys. Rev. B **64**, 125420 (2001).
[22] J. C. Maxwell-Garnett, Philos. Trans. R. Soc. London, Ser. A **203**, 385 (1904); **205**, 237 (1906).
[23] D. A. G. Bruggemann, Ann. Phys. **24**, 636 (1935).
[24] U. Kreibig and M. Vollmer, *Optical Properties of Metal Clusters*, Springer Series in Material Science, 25 (Springer-Verlag, Berlin, 1995).
[25] G. A. Farias, E. F. Nobre, R. Moretzsohn, N. S. Almeida, and M. G. Cottam, J. Opt. Soc. Am. A **19**, 2449 (2002).
[26] J. L. Menéndez, B. Bescos, G. Armelles, R. Serna, J. Gonzalo, R. Doole, A. K. Petford-Long, and M. I. Alonso, Phys. Rev. B **65**, 205413 (2002).